Artificial Neural Network-Based Hybrid Controller for Electric Vehicle Applications

RAKESH BABU BODAPATI*, R. S. SRINIVAS, P. V. RAMANA RAO
Department of Electrical and Electronics Engineering,
Acharya Nagarjuna University,
Guntur, Andhra Pradesh-522510
INDIA

**Corresponding Author*

Abstract: - Power management among different energy sources of electric vehicles (EV) is one of the complex issues during the transition from one to another. A specific control is modeled based on the current and speed range of the electric motor named as Measurement of Parameter-Based Controller (MPBC), which will play a key role during transition of energy sources as per the load requirement. Two bidirectional converters are utilized to control the pulse signals generated by the traditional controllers which are connected at the battery and Supercapacitors (SCap) ends, which are treated as passive sources of the system. The Controller's artificial neural network (ANN), fuzzy logic (FLC), and proportional-integral (PI) are utilized to generate the pulse signal to the switches present in the converters by load. Further, specific controller MPBC is combined with three controllers ANN/FLC/PI individually and obtained three separate hybrid controllers as per the proposed control technique. The MPBC+PI/FLC/ANN controller-based MATLAB/Simulink model was designed, and applied to the electric motor individually at different load conditions. This model considered three different power delivery states from the PV array and assessed the motor's performance under different load scenarios. Compare the three hybrid controllers' final results to find out which one is more effective than the others.

Key-Words: - Artificial Neural Network (ANN), Photo Voltaic (PV) energy, Fuzzy Logic System, Super Capacitor, Proportional Integral (PI) controller, Hybrid controller (HC), Measurement of parameter-based controller (MPBC), Electric vehicle, Battery.

Received: April 23, 2024. Revised: August 27, 2024. Accepted: September 25, 2024. Published: October 31, 2024.

1 Introduction

An eco-friendly and sustainable substitute for traditional energy sources like nuclear power and fossil fuels is solar power generation. Due to the abundant and endless supply of sunlight, one of the main benefits of solar electricity is that it is renewable. Solar energy is a clean and sustainable energy source since it produces no greenhouse gas emissions, in contrast to fossil fuels. On the other hand, traditional energy sources such as coal, oil, and natural gas are limited resources that need to be extracted and processed, resulting in greenhouse gas emissions and damage to the environment. Significant dangers to the environment and human health are additionally created by these sources, including habitat destruction, air and water pollution, and climate change.

Photovoltaic (PV) panels and concentrated solar power (CSP) plants are examples of solar power generation systems that use the sun's energy to create electricity. Decentralized and distributed energy solutions can be achieved by integrating them into building materials, solar farms, and rooftop deployments. Furthermore, as a result of improvements in efficiency as well as cost generated by solar technology, solar power is now more affordable and accessible than conventional energy sources, [1]. In general, solar energy has many advantages over traditional energy sources, such as lower carbon emissions, long-term cost savings, energy independence, and environmental sustainability. It is essential to switch to clean and renewable energy sources in the future, [2].

FLC-based tracking system. Different types of camera tracking controllers have been developed based on the FLC also tested in simulation software. In this the pixel positions from the image are taken as input on the other hand provided pan will be considered as output. Two types of rules-based tuning technique is applied to the membership functions to obtain the better-quality picture from the camera, [3].

In [4], an FLC for autonomous vehicle propulsion. The FLC can control the speed of the vehicle on its own based on the load. The range of the heading range is taken and given to the FLC for proper operation of the vehicle. The noise analysis of the controller was also performed to attain the importance of other controllers' performance.

Stated the effect of the FLC on the sliding mode control technique applied to the various speed-controlling applications. The sliding mode control (SMC) generally requires the all data of the plant model. On the other hand, the FLC is more robust than the SMC. In this, the effect of the FLC is investigated on the SMC and executed with all simulation results, [5]. Developed an automatic system with FLC. The automatic transmission (AT) system for the vehicle propulsion is one of the useful factors for the vehicle. Generally, a mechanical gear system is used in conventional transport vehicles, the driver is required to change the gear depending on the vehicle condition. An FLC-based gear system is designed and implemented for the vehicles for better performance, [6], [7], [8].

Proposed the NN-based technique for fast convergence and accuracy [9]. In this, a procedure is developed to train ANN for effective control. This type of system gives better results after completion of the successful training. Especially, feedforwarded NN is developed to know the performance of the non-linear components or systems, [10]. A statistical-based algorithm was also developed, to examine the performance of the ANN technique. At each iteration a new network is modelled to remove the previously occurred errors. The intended approach is rapidly applicable where a large amount of trained data can be produced, [11].

An NN-based dynamic simulation of the suspension for irregular road conditions, [12]. The NN is trained from the validation data obtained from the laboratory. The results obtained from NN show the effectiveness for a wide range of applications. This has been applied to the vehicle based on the elastic bushings and dynamics of the tire. And this NN-based model is very much useful for assessing vehicle ride, vibration, and noise because of its better computational efficiency and accuracy, [13].

Introduced an ANN controller for maximum power point tracking (MPPT), [14]. The ANN control with an MPPT is applied to the boost converter to attain the high efficiency and the reference voltage is obtained for ANN from MPPT. The adopted technique will change the PV module voltage as per the MPPT instruction at any temperature, or insulation. To attain an effective response from the proposed model, the system is implemented with a digital signal processor (DSP). The overall information obtained from the system is applied to the ANN to generate the duty cycle as per the load requirement, [15].

[16], Stated control technique to the HEV based on the ANN to improve the effectiveness of the AC/DC converters. The switches in the Series HEV are exposed to open conditions because the internal problems that occurred during the operation. The ANN-based controller is used to identify the switching problem at various levels, and various patterns are considered. The intended control technique is implemented in simulation and also validated through a small experimental setup, [17].

An effective braking system corresponding to HESS for EVs, HEVs, and PHEV with BLDC motor is proposed. Different character batteries and UC are combined for HESS for better utilization of the battery and also charging of UC from the regenerative braking system (RGS), at this time the BLDC acts as a generator. Using a proper controlling algorithm, the voltage is boosted, sent to the UC or battery. The crest power is useful for avoiding the complete discharge of the battery during the uphill of the vehicle. The ANN-based technique is used here to attain smooth breaking distribution, [18].

The EV charge scheduling using ANN is illustrated. The machine-to-machine (M2M) plays a vital role if the EVs are integrated with the power grid for charging of the power source, here energy management is one of the key factors to control. The smart devices connected to the system will predict the power demand and supply needs of the system. In this case, ANN-based algorithm is used for EVs charging schedule by taking data from M2M. The household data generally used to decide the charging schedule of the vehicle, [19].

An ANN for instant power development of the EVs. In this, the accuracy of the instant power has been increased to estimate the power the battery-powered vehicles are developed. In general, the battery can be utilized as a secondary power source or main source in the EV application depending upon the requirement. The power source characteristics are identified from the SOC, voltage, and health of the device. The ANN is used here for estimating the instant power to the EV for better efficiency, [20].

2 Artificial Neural Network

The NN (Neural Network) controller, using the Backpropagation (BPN) algorithm, uses

reinforcement-type learning to self-tune its parameters to allow it to follow a specified trajectory. When dealing with control difficulties in the real world, it is usual to draw on extensive past knowledge about different subsystems of control systems. This abundance of data improves the accuracy and dependability of Neural Networks (NNs) used to simulate these subsystems. With the help of extensive data, NNs may be trained to precisely reflect and imitate the behavior of complex plants, leading to enhanced performance in control applications.

The goal of a self-learning computational system integrates the closely related fields of neural networks, parallel processing, connectionism, and neural computing. Neural networks are based on the neuron, a basic building block that makes complicated learning and decision-making possible. Neurons are the processing elements of neural networks. These simple elements are connected by a variety of topological classes, trained by yet another class of learning algorithms.

2.1 Backpropagation Principles of Operation

The BPN neural network belongs to the class of feedforward networks. This implies that information flows in one direction only - from input to output. The multilayered feedforward neural network can learn a mapping of any complexity. The network's learning of a particular pattern is based on repeated presentation of the data set. This type of neural network has a propagate-adjust cycle allowing the neural network to learn an entire data set. The data set is presented to the inputs of the neural network and the information travels through the hidden layer to the output layer. This action constitutes the propagation phase. The adjust stage entails the comparison of these outputs to desired outputs, and the error information is to modify the weights of the neural network. This error BPN is the basis for the training algorithm used to train a multilayered feedforward network.

2.2 Backpropagation Structure and Components

The BPN is one of the many existing neural network topologies. It is composed of several nodes at which point computation takes place. This node or neuron is the basic building block upon which the neural network structure is built It is intended to simulate a biological neuron.

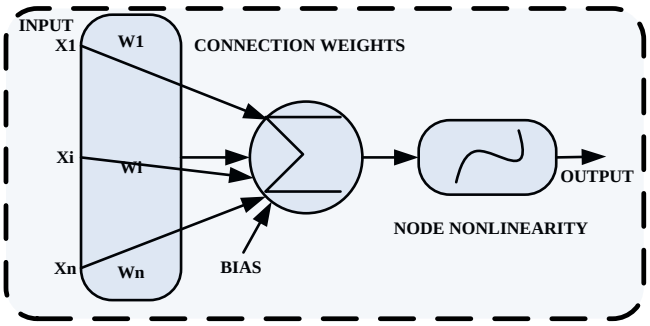

Fig. 1: Basic Neuron model

The Backpropagation Neural Network (BPN) neuron model shown in Figure 1 has several inputs and one output. Every input contributes to the total output after going through a connection weight Wn. The inputs, the associated weights of the inputs, a bias term, and a squashing function—which adds non-linearity to the node—all decide the output. By modifying weights and biases during training, this structure helps the BPN understand complex data patterns, improving its capacity for learning and precise forecasting.

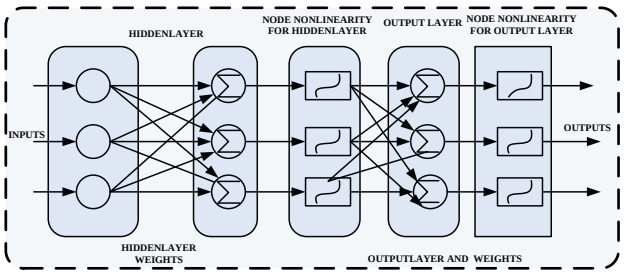

Fig. 2: General BPN NN structure

The basic backpropagation structure is composed of layers of these interconnected neurons as shown in Figure 2. The network is made up of three distinct layers. The input layer serves as an interface with the connecting system. It directly feeds the hidden layer via a network of connection weights. Since the hidden layer is built from the neuron model it takes the sum of al1 the inputs and a bias. This sum known as neth is then passed through a nonlinear function. This result flows through the interconnecting weights to the output layer where the summing process starts all over again. The error terms between the desired output and the network output are calculated and used to adjust the output weights and then propagated back to contribute to the process for al1 the hidden layer weights. The net continues in this propagate-adjust manner until all patterns are learned.

2.3 Backpropagation Governing Equations

The equation governing the operation of the BPN shown in Figure will now be presented. The input to the hidden layer is:

$$neth_{pj} = \sum_{i=1}^{N} (wh_{ji} * x_{pi}) + \theta h_j \quad (1)$$

The weight connections between the input and the hidden layer are denoted as Whg and &θhji is a bias input. The use of the bias input is optional. These are then processed by a squashing function:

$$Y_{pj} = Fh_j(neth_{pj}) \quad (2)$$

The outputs of these hidden nodes become the inputs to the output layer. Thus,

$$neto_{pk} = \sum_{j=I}^{L} \left(wo_{kj} * Y_{pj} \right) + \theta o_k \quad (3)$$

where the connections between the hidden layer and the output layer are denoted as wo_{kj} and θo_k is the bias input. These outputs must also be treated by a squashing function. This results in an output of:

$$O_{pk} = FO_k(neto_{pk}) \quad (4)$$

The next step will be to describe the delta update rule. The backpropagation algorithm performs the steepest descent minimization on a surface in weight space whose height at any point is equal to the error.

The error between the actual net output and the target is defined as:

$$E_k = (d_k - O_k) \quad (5)$$

For the network to learn this error must be minimized and used in some way to update the weights in the output layer as well as those associated with the hidden layer. The following error is defined.

$$E_p = \frac{1}{2} * \left[\sum_k \left(Tp_k - O_{pk} \right)^2 \right] \quad (6)$$

And

$$\frac{\partial E_p}{\partial wo_{kj}} = -\left(T_{pk} - O_{pk} \right) * \frac{\partial Fo_k}{\partial neto_{pk}} * \frac{\partial neto_{pk}}{\partial wo_{kj}} \quad (7)$$

$$\frac{\partial neto_{pk}}{\partial wo_{kj}} = \frac{\partial}{\partial wo_{kj}} * \sum_j \left(wo_{kj} * Y_{pj} + \theta o_k \right) \quad (8)$$

$$\frac{\partial E_p}{\partial wo_{kj}} = -\left(T_{pk} - O_{pk} \right) * \frac{\partial Fo_k}{\partial neto_{pk}} * Y_{pj} \quad (9)$$

The above equation allows for a weight update rule of the following form:

$$wo_{kj}(t+1) = wo_{kj}(t) + \eta * (T_{pk} - O_{pk}) * Fo_k(neto_k) * Y_j \quad (10)$$

Letting

$$\delta o_{pk} = (T_{pk} - O_{pk}) * Fo_k(neto_{pk}) \quad (11)$$

we have for the output layer

$$wo_{kj}(t+1) = wo_{kj}(t) + \eta * \delta o_{pk} * Y_{pj} \quad (12)$$

and smeller for the hidden layer

$$\delta h_{pj} = F_{hj}(neth_{pj}) * \sum \left(\delta o_{pk} * wh_{kj} \right) \quad (13)$$

$$wh_{ji}(t+1) = wh_{ji}(t) + \eta * \delta h_{pj} * X_i \quad (14)$$

where the derivative of the squashing function is needed for both the hidden layer as well as the output layer. Here we can see the algorithm's dependency upon the error terms computed for the output layer as well as the hidden layer. The above-described equations are a basis for the following study of some modifications on the generalized delta rule backpropagation networks.

3 A Proposed Control Technique for Energy Management Strategy

This suggests a novel control technique called SCap to allow the battery to alternate between its charging and discharging cycles based on the speed and current values of the electric motor. The recommended control technique is implemented using three different hybrid controllers; the traditional controllers, ANN, FLC, and PI, are utilized to generate the pulse signals that are transmitted to the converter. Furthermore, the MPBC controller regulates these signals based on the speed and current levels of the electric motor. Ultimately, the combination of MPBC+PI, MPBC+FLC, and MPBC+ANN provides the method to implement the recommended procedure.

The main circuit of the proposed model consists of up of the PV array, battery, SCap, two bidirectional converters, Boost converter, and electric motor which are depicted in Figure 3. In this instance, the SCap is utilized to meet the peak power consumption, and the battery powers the EV

if solar power generation is unavailable. On the other hand, PV arrays are employed to meet the demand for EVs as well as for battery and SCap charging, depending on the load placed on the EV. The three different controller combinations known as MPBC plus PI/FLC/ANN constitute the suggested control technique, which is the base for all of the regulated signals of the two bidirectional converters. In this case, the PI, FLC, or ANN controller generates the pulse signal to the converter at the battery and SCap end based on the actual and reference voltage levels of the converter. But MPBC functions according to the current and speed readings of the EM. This is accomplished by using mathematical functions, which, based on the current and speed values of the EM, generate several different types of signals. MPBC, PI, FLC, and ANN combine to supply the EV with the proper power supply based on the applied load, supplying the converter at the battery and SCap ends with controlled pulse signals.

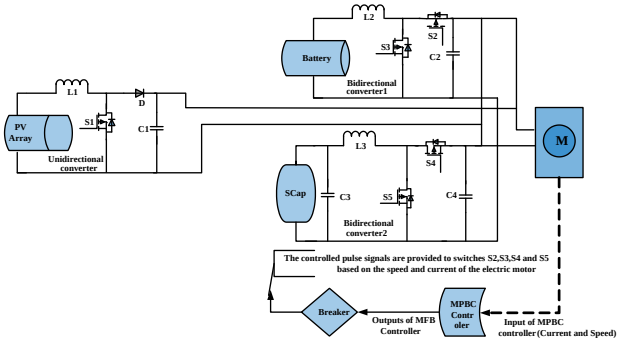

Fig. 3: Main circuit with a Proposed control technique

4 MATLAB/Simulation Results and Discussions

In this case, the controlled signals to the EV are designed considering three different load conditions. This will take place in line with the recommended controlled approach, which blends MPBC, ANN, FLC, and PI.

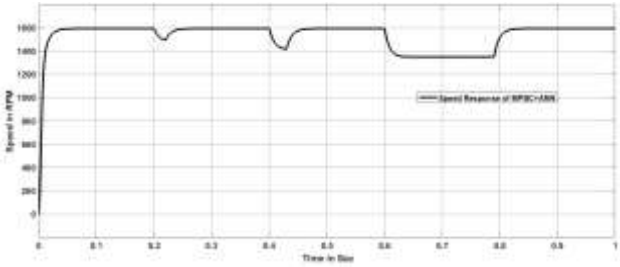

Fig. 4: Speed response of the electric motor with MPBC+ANN Controller

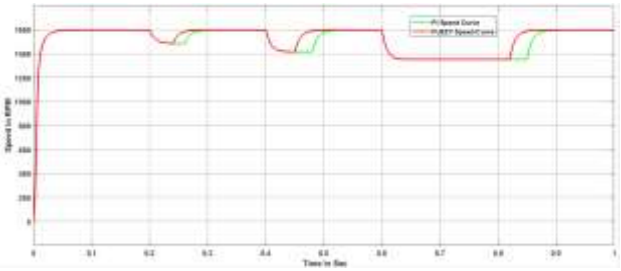

Fig. 5: Speed response of the electric motor with MPBC+FLC and MPBC+PI Controllers

The speed curve response of EM under varied loads is displayed in Figure 4 and Figure 5. To verify the effectiveness of the recommended control strategy, three different loads are applied to the EV at three different times. The motor slows to roughly 1500 rpm when a standard load is put to the EM for 0.2 seconds. In 0.4 seconds, the motor drops to 1400 rpm when a rated load is applied. Finally, the motor's speed drops to even less than 1400 rpm when an additional 0.6-second rated load is introduced. MPBC+PI took 0.09 seconds, 0.1 seconds, and 0.30 seconds, MPBC+ANN took 0.05 seconds, 0.07 seconds, and 0.21 seconds, and MPBC+FLC took 0.075 seconds, 0.08 seconds, and 0.28 seconds to reach stable with the applied loads in that order. MPBC with ANN improved the other controller output, according to the results.

4.1 Mode-I Operation (PV Active Case)

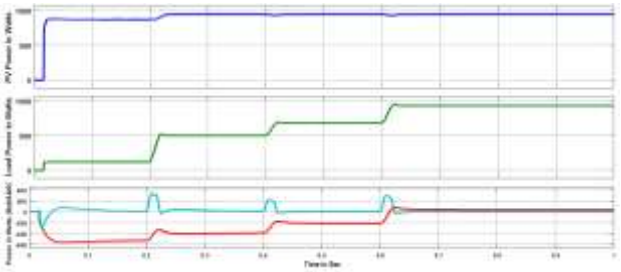

Fig. 6: Representation of the PV, Load & Battery, SCap Power curves, related PV active case

In this mode of operation, PV is able to supply power to the load along with the battery and SCap changing (for a short period). Figure 6 shows the power curves of the load, passive source, and active source PV.

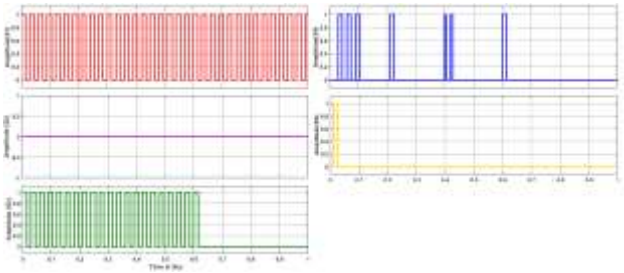

Fig. 7: Representation of the pulse signals of the five switches of the complete circuit, related PV active case

Figure 7 shows the pulse signal generation of the 5 switches present in the circuit, this mode of operation S1having the continues pulses which shows that the PV array is supplying power throughout the time as specified, S2 is used in the converter at battery end used for boost operation (discharging) no signal found which shows the no output provided from the battery, S3 is used for buck operation of the converter at battery end, as per the Figure 7 shows the pulse signals up to 0.6 sec which shows the battery charging period. Switches S4 and S5 are used in the bidirectional converter used at SCap, here S4 is for boost operation and S5 is for buck operation, it is clear when ever load applied to the EM SCap can discharge to meet the instance power requirement of the load.

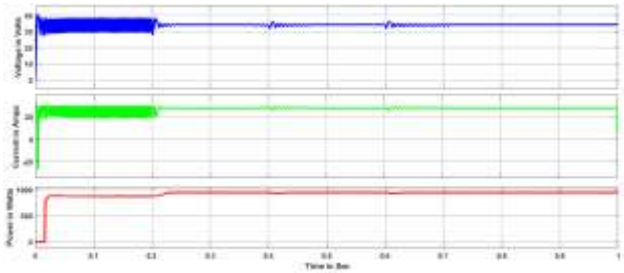

Fig. 8: Representation of the PV array voltage, current and power curves, related PV active case

In this mode of operation total power is supplied by the PV array which is required by the two passive sources and the load which is clear in Figure 8.

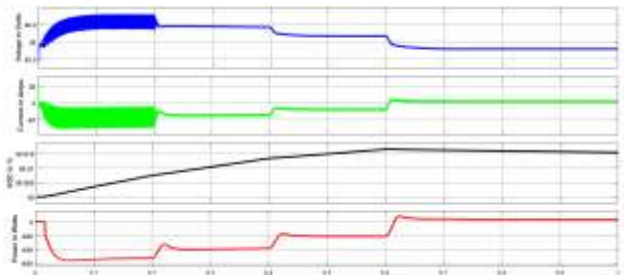

Fig. 9: Representation of the Battery voltage, current, %SOC and power curves, related PV active case

Figure 9 shows the battery parameters-related representation. In this case, power consumed by the battery shows with negative region, even current values also.

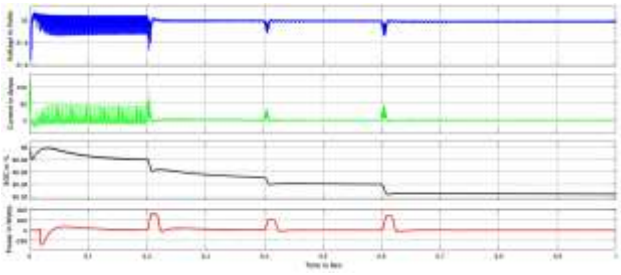

Fig. 10: Representation of the SCap voltage, current, %SOC, and power curves, related PV active case

Figure 10 shows the SCap parameters, the power becomes negative during the starting of the motor, further all load-applied cases power curve shows the positive gesture corresponding to that voltage, % SOC, and current values are also changed.

4.2 Mode-II Operation (PV and Battery Active Case)

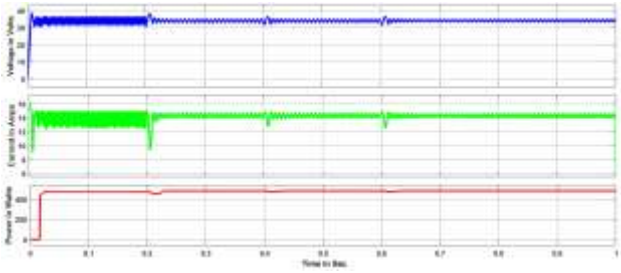

Fig. 11: Representation of the PV, Load & Battery, SCap Power curves, related PV and Battery active case

In this mode of operation PV can supply 50% of the power to the load along and remain part can be sent from the battery which clearly from Figure 11 shows the power curves of the load, passive source, and active source PV.

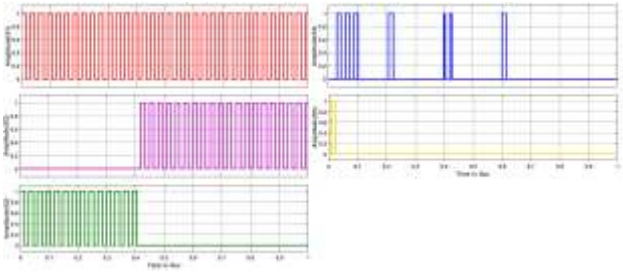

Fig. 12: Representation of the pulse signals of the five switches of the complete circuit, related PV, and Battery active case

Figure 12 shows the pulse signal generation of the 5 switches present in the circuit, this mode of operation S1having continuous pulses which show that the PV array is supplying power throughout the time as specified, S2 is used in the converter at battery end used for boost operation (discharging) signals found from 0.4 sec onwards, S3 is used for buck operation of the converter at battery end, as per the Figure 12 shows the pulse signals up to 0.4 sec which shows the battery charging period. Switches S4 and S5 are used in the bidirectional converter used at SCap, here S4 is for boost operation and S5 is for buck operation, and it is clear whenever load applied to the EM SCap can discharge to meet the instance power requirement of the load.

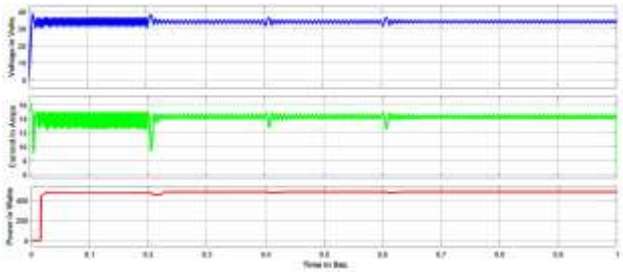

Fig. 13: Representation of the PV array voltage, current and power curves, related PV, and Battery active case

In this mode of operation total power is supplied by the PV array which is required by the two passive sources and the load which is clear in Figure 13 and 50% of the load requirement is done thorough PV array.

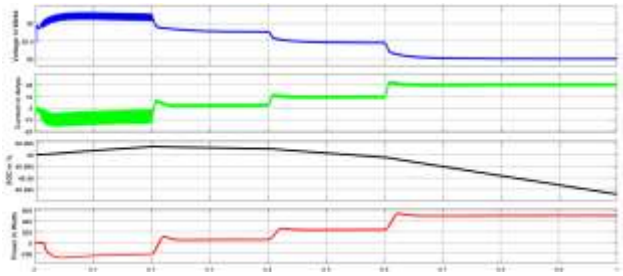

Fig. 14: Representation of the Battery voltage, current, %SOC and power curves, related PV, and Battery active case

The representation connected to battery parameters is shown in Figure 14. In this instance, both the battery's power consumption and its current values are negative.

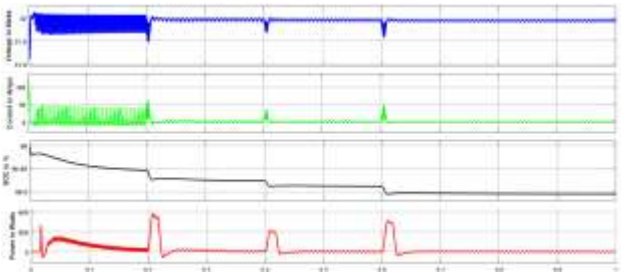

Fig. 15: Representation of the SCap voltage, current, %SOC and power curves, related PV, and Battery active case

Figure 15 displays the SCap parameters. The power decreases when the motor starts, and in all load-applied scenarios, the power curve displays a positive gesture that corresponds to changes in voltage, percentage SOC, and current values.

4.3 Mode-III Operation (Battery Active Case)

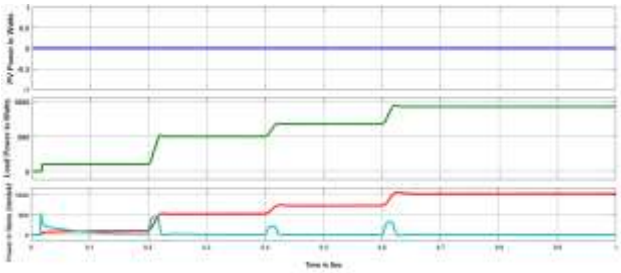

Fig. 16: Representation of the PV, Load & Battery, SCap Power curves, related Battery active case

In this mode of operation, no power flows are there from PV, and all required power is sent from the battery which is clear from Figure 16 shows the power curves of the load, passive source.

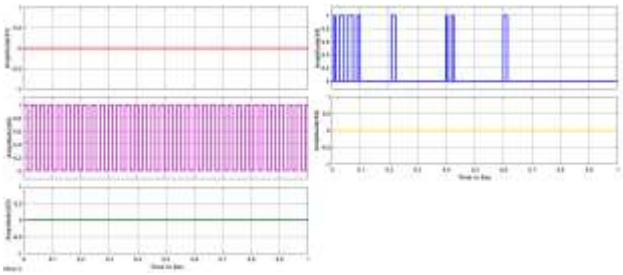

Fig. 17: Representation of the pulse signals of the five switches of the complete circuit, related Battery active case

Figure 17 shows the pulse signal generation of the 5 switches present in the circuit related to no power supplied from the PV array case. Here no pulse signal generation there for switch S1 since no sunlight condition. Further, all power needed by the load is provided by the battery with the help of the

SCap during peak power requirement which enables the signal switches signals of the S2 and S4 for boost operation at the battery, SCap end.

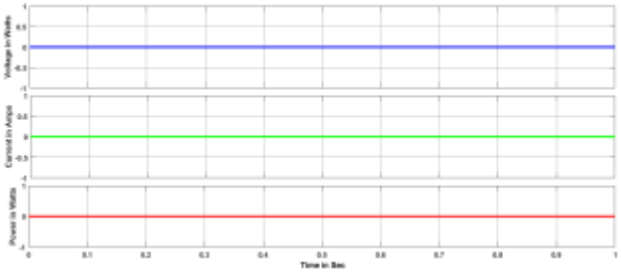

Fig. 18: Representation of the PV array voltage, current and power curves, related Battery active case

Figure 18 shows the no parameters available case from the PV array since no sunlight condition and shows all values as zero.

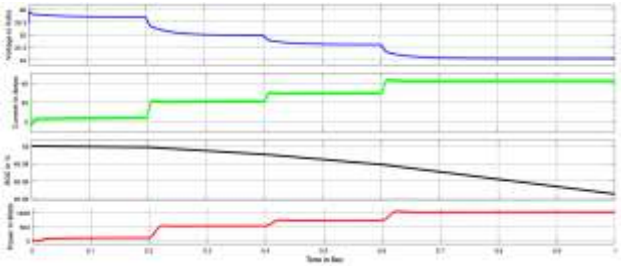

Fig. 19: Representation of the Battery voltage, current, %SOC, and power curves, related Battery active case

The representation connected to battery parameters is shown in Figure 19. In this instance, both the battery's power and current numbers display a positive region.

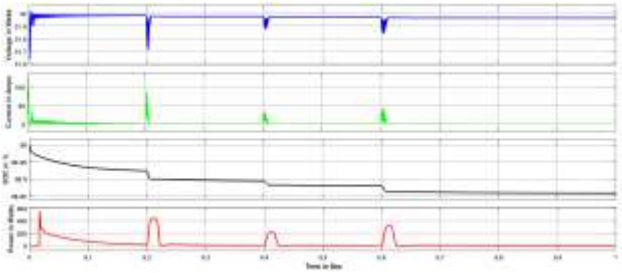

Fig. 20: Representation of the SCap voltage, current, %SOC, and power curves, related Battery active case

Figure 20 displays the SCap characteristics. When the motor is first started, the power turns negative. When a load is supplied, the power curve also displays a positive gesture that corresponds to changes in voltage, percentage SOC, and current values.

Table 1. Based on the speed value, a performance comparison is made between MPBC plus PI and MPBC plus FLC, MPBC plus ANN.

S. No	Controller Name	Time Taken to reach Steady state in sec		
		Mode1	Mode2	Mode3
1	MPBC+PI	0.09	0.1	0.30
2	MPBC+FLC	0.075	0.08	0.28
3	MPBC+ANN	0.05	0.07	0.21

Based on the speed curve settling value, Table 1 shows the comparison analysis of MPBC with PI, FLC, and ANN. Moreover, MPB plus ANN excelled with MPBC plus PI/FLC in terms of performance.

5 Conclusion

This study looks at a control system that adjusts the battery and SCap about the motor's speed. The MPBC is the result of combining three distinct mathematical functions that are independently realized based on the motor's speed and current values. To achieve the main objective of the research, the suggested MPBC controller is integrated with a conventional PI controller, FLC, and ANN to form a hybrid controller. While the PI controller, FLC, and ANN produced the switching signals required by the converter, the MFBC controlled the pulse signals that correlated with the motor speed. In the final analysis, the requirements of electric vehicles are fulfilled by employing the recommended control strategy, which results in a smooth transition between battery and SCap. Another hybrid controller, termed MPBC with ANN, is designed to perform the same purpose as MFBC plus FLC. A comparative analysis is done before applying the afterload and proceeding. The results for both approaches are tabulated and presented in the final section. In the end, the MPBC plus ANN outperformed the MPBC+PI and MPBC+FLC hybrid controllers in terms of performance.

References:

[1] S. M. Shariff, M. S. Alam, F. Ahmad, Y. Rafat, M. S. J. Asghar and S. Khan, (2020). "System Design and Realization of a Solar-Powered Electric Vehicle Charging Station," in *IEEE Systems Journal*, vol. 14, no. 2, pp.

2748-2758, doi: 10.1109/JSYST.2019.2931880.

[2] M. H. Mobarak, R. N. Kleiman and J. Bauman (2021). "Solar-Charged Electric Vehicles: A Comprehensive Analysis of Grid, Driver, and Environmental Benefits," in *IEEE Transactions on Transportation Electrification*, vol. 7, no. 2, pp. 579-603, doi: 10.1109/TTE.2020.2996363.

[3] D. Phan, A. Bab-Hadiashar, M. Fayyazi, R. Hoseinnezhad, R. N. Jazar and H. Khayyam (2021), "Interval Type 2 Fuzzy Logic Control for Energy Management of Hybrid Electric Autonomous Vehicles," in *IEEE Transactions on Intelligent Vehicles*, vol. 6, no. 2, pp. 210-220, doi: 10.1109/TIV.2020.3011954.

[4] B. Sah, P. Kumar and S. K. Bose (2021), "A Fuzzy Logic and Artificial Neural Network-Based Intelligent Controller for a Vehicle-to-Grid System," in *IEEE Systems Journal*, vol. 15, no. 3, pp. 3301-3311,doi: 10.1109/JSYST.2020.3006338.

[5] M. Suhail, I. Akhtar, S. Kirmani and M. Jameel (2021), "Development of Progressive Fuzzy Logic and ANFIS Control for Energy Management of Plug-In Hybrid Electric Vehicle," in *IEEE Access*, vol. 9, pp. 62219-62231, doi: 10.1109/ACCESS.2021.3073862.

[6] J. Li, Q. Zhou, H. Williams and H. Xu (2020), "Back-to-Back Competitive Learning Mechanism for Fuzzy Logic Based Supervisory Control System of Hybrid Electric Vehicles," in *IEEE Transactions on Industrial Electronics*, vol. 67, no. 10, pp. 8900-8909, doi: 10.1109/TIE.2019.2946571.

[7] G. C. Lazaroiu and M. Roscia (2022), "Fuzzy Logic Strategy for Priority Control of Electric Vehicle Charging," in *IEEE Transactions on Intelligent Transportation Systems*, vol. 23, no. 10, pp. 19236-19245, doi: 10.1109/TITS.2022.3161398.

[8] Hayat El Aissaoui, Abdelghani El Ougli, Belkassem Tidhaf (2022). MPPT Using PSO Technique Comparing to Fuzzy Logic and P&O algorithms for Wind Energy Conversion System. *WSEAS Transactions on Systems and Control*. vol. 17, pp.305-313, https://doi.org/10.37394/23203.2022.17.35.

[9] Katuri, R., Gorantla, S. (2020). Optimal performance of lithium-ion battery and ultra-capacitor with a novel control technique used in E-Vehicles. *Journal of New Materials for Electrochemical Systems*, Vol. 23, No. 2, pp. 139-150, doi: 10.14447/jnmes.v23i2.a11.

[10] S. Arandhakar, N. Jayaram, Y. R. Shankar, Gaurav, P. S. V. Kishore and S. Halder (2022), "Emerging Intelligent Bidirectional Charging Strategy Based on Recurrent Neural Network Accosting EMI and Temperature Effects for Electric Vehicle," in *IEEE Access*, vol. 10, pp. 121741-121761, doi: 10.1109/ACCESS.2022.3223443.

[11] A. A. Hussein (2019), "Adaptive Artificial Neural Network-Based Models for Instantaneous Power Estimation Enhancement in Electric Vehicles' Li-Ion Batteries," in *IEEE Transactions on Industry Applications*, vol. 55, no. 1, pp. 840-849, doi: 10.1109/TIA.2018.2866102.

[12] Bin Xu;Xiaosong Hu;Xiaolin Tang;Xianke Lin;Huayi Li;Dhruvang Rathod;Zoran Filipi (2020)., "Ensemble Reinforcement Learning-Based Supervisory Control of Hybrid Electric Vehicle for Fuel Economy Improvement," in *IEEE Transactions on Transportation Electrification*, vol. 6, no. 2, pp. 717-727. doi: 10.1109/TTE.2020.2991079.

[13] Katuri, R., & Gorantla, S. (2020). Realization of prototype hardware model with a novel control technique used in electric vehicle application. *Electrical Engineering*, 102(4), 2539-2551, doi: 10.1007/s00202-020-01052-0.

[14] Shen, J., & Khaligh, A. (2015). A supervisory energy management control strategy in a battery/ultracapacitor hybrid energy storage system. *IEEE Transactions on transportation electrification*, 1(3), 223-231, doi: 10.1109/TTE.2015.2464690.

[15] Cao, J., & Emadi, A. (2011). A new battery/ultracapacitor hybrid energy storage system for electric, hybrid, and plug-in hybrid electric vehicles. *IEEE Transactions on power electronics*, 27(1), 122-132, doi: 10.1109/TPEL.2011.2151206.

[16] Chiheb Ben Regaya, Fethi Farhani, Hichem Hamdi, Abderrahmen Zaafouri, Abdelkader Chaari (2020). Robust ANFIS Vector Control of Induction Motor Drive for High-Performance Speed Control Supplied by a Photovoltaic Generator. *WSEAS Transactions on Systems and Control*. vol. 15, pp.356-365, https://doi.org/10.37394/23203.2020.15.37.

[17] Khaldi Hamza, Mounir Hamid, Boulakhbar Mouaad (2022). A Review of Future Fuel Cell Electric Vehicles and Challenges Related to Morocco. *WSEAS Transactions on Power Systems.* vol. 17, pp.339-353, https://doi.org/10.37394/232016.2022.17.34.

[18] X. Li and S. Wang (2021), "Energy management and operational control methods for grid battery energy storage systems," *in CSEE Journal of Power and Energy Systems*, vol. 7, no. 5, pp. 1026-1040, doi: 10.17775/CSEEJPES.2019.00160.

[19] Ning Yan; Yao Zhong; Xiangjun Li; Yulong Wang; Longtao Su; Wan Jiang; Jianxiang Zhou (2021), "Energy Management Method of Electricity Heat Hydrogen Multi-Coupling System for Retired Power Battery Echelon Utilization in Microgrids," *in IEEE Transactions on Applied Superconductivity*, vol. 31, no. 8, pp. 1-5, doi: 10.1109/TASC.2021.3110471.

[20] Mostafa M. E. F. Shams, Hosam Abd El- Aziz Amr, Rania Rushdy Moussa (2021). Comparative Analysis on the Effects of Natural & Artificial Indoors Lighting on the Learning and Interactive Process. *WSEAS Transactions on Power Systems*. vol. 16, pp.121-127, https://doi.org/10.37394/232016.2021.16.12.

Contribution of Individual Authors to the Creation of a Scientific Article (Ghostwriting Policy)

The authors equally contributed in the present research, at all stages from the formulation of the problem to the final findings and solution.

Sources of Funding for Research Presented in a Scientific Article or Scientific Article Itself

No funding was received for conducting this study.

Conflict of Interest

The authors have no conflicts of interest to declare.